

Renormalization of the Unitary Evolution Equation for Coined Quantum Walks

Stefan Boettcher¹, Shanshan Li¹, and Renato Portugal²

¹*Department of Physics, Emory University, Atlanta, GA 30322; USA*

²*Laboratório Nacional de Computação Científica, Petropolis, RJ 25651-075; Brazil*

We consider discrete-time evolution equations in which the stochastic operator of a classical random walk is replaced by a unitary operator. Such a problem has gained much attention as a framework for coined quantum walks that are essential for attaining the Grover limit for quantum search algorithms in physically realizable, low-dimensional geometries. In particular, we analyze the exact real-space renormalization group (RG) procedure recently introduced to study the scaling of quantum walks on fractal networks. While this procedure, when implemented numerically, was able to provide some deep insights into the relation between classical and quantum walks, its analytic basis has remained obscure. Our discussion here is laying the groundwork for a rigorous implementation of the RG for this important class of transport and algorithmic problems, although some instances remain unresolved. Specifically, we find that the RG fixed-point analysis of the classical walk, which typically focuses on the dominant Jacobian eigenvalue λ_1 , with walk dimension $d_w^{RW} = \log_2 \lambda_1$, needs to be extended to include the subdominant eigenvalue λ_2 , such that the dimension of the quantum walk obtains $d_w^{QW} = \log_2 \sqrt{\lambda_1 \lambda_2}$. With that extension, we obtain analytically previously conjectured results for d_w^{QW} of Grover walks on all but one of the fractal networks that have been considered.

I. INTRODUCTION

Quantum walks present one of the frameworks for which quantum computing can satisfy its promise to provide a significant speed-up over classical computation. Grover [1] has shown that a quantum walk can locate an entry in an unordered list of N elements (i.e., sites in some network) in a time that scales as $\sim \sqrt{N}$, a quadratic speed-up over classical search algorithms. However, that finding was based on a list in which all elements are interconnected with each other, thus, raising the question regarding the impact of geometry on this result. Note, for instance, that if the walk had to pass the list over a linear, $1d$ -line of sites, no quantum effect would provide an advantage over simply passing every site until the desired entry is located. And for obvious engineering reasons, the design of a quantum algorithm that could satisfy the Grover limit for lists embedded in $2d$ -space is particularly desirable. Here, the issue of geometry is especially pertinent, as it has been shown that only discrete-time quantum walks with internal degrees of freedom (e.g., “coined” walks) can attain the Grover-speedup for search on lattices with $d \leq 4$ [2–5]. Our discussion here is focused on the long-time asymptotic properties of such coined quantum walks.

While less dramatic as the super-polynomial speed-up of Shor’s algorithm for factoring [6], searching is a far more common [7] and equally important task in the age of search engines [8, 9]. As fundamental as the random walk is to the description of randomized algorithms in computer sciences [7, 10], likewise quantum walks have been established as a universal model of quantum computing [11, 12]. Aside from their algorithmic relevance, the *physical* behavior of quantum walks, their entanglement, localization, and interference effects [13–17] in spe-

cific environments, rivals classical diffusion as an important transport problem [18, 19]. Already, there are numerous experimental realizations of quantum walks, such as in wave-guides [20, 21], photonics [22, 23], and optical lattices [24].

Whether we talk about random or about quantum walks, a complete description for the spreading behavior is provided by the probability density function (PDF) $\rho(\vec{x}, t)$ to detect a walk at time t at site of distance $x = |\vec{x}|$ after starting at the origin. For random walks at large times and spatial separations, the PDF obeys the scaling collapse with the scaling variable $x/t^{1/d_w}$,

$$\rho(\vec{x}, t) \sim t^{-\frac{d_f}{d_w}} f\left(x/t^{\frac{1}{d_w}}\right), \quad (1)$$

where d_w is the walk-dimension and d_f is the fractal dimension of the network [25]. On a translationally invariant lattice in any spatial dimension $d(=d_f)$, it is easy to show that the walk is always purely “diffusive”, $d_w = 2$, with a Gaussian scaling function f . The scaling in Eq. (1) still holds when translational invariance is broken in certain ways or the network is fractal (i.e., d_f is non-integer). However, anomalous diffusion with $d_w \neq 2$ may arise in many of those transport processes [18, 25–27]. This scaling affects many important observables, for instance, the mean-square displacement, $\langle x^2 \rangle_t \sim t^{2/d_w}$, or first-passage times [19, 28, 29].

We stipulate that a scaling relation like Eq. (1) holds also for the coined quantum walk we are discussing in this paper. For walks on regular lattices, Eq. (1) indeed applies in the “weak limit”, but simply with $d_w^{QW} = 1$ [30, 31]. Beyond the regular lattice, the renormalization group (RG) is a good method to explore the asymptotic scaling of a walk [19, 25, 27]. Elucidating the effects of geometry and internal symmetries is exactly the task that the real-space Renormalization group (RG) has been

invented for in the context of critical scaling in statistical physics [32, 33]. Indeed, the RG of classical random walks provides a straightforward blueprint for developing the RG for a quantum walk, even with the added complication of an internal coin space [34]. In this way, exact RG-flow equations for quantum walks on a number of complex networks have been derived [15, 16]. Those results, for instance, have led to the conjecture that the walk dimension d_w in Eq. (1) for a quantum walk with a Grover coin always is *half* of that for the corresponding random walk, $d_w^{QW} = \frac{1}{2} d_w^{RW}$ [16].

Unlike for the classical case, however, the analysis of the RG-flow for quantum walks had only been conducted numerically, albeit with high precision. The main obstacle for a rigorous treatment, and its (partial) resolution we present here, is briefly stated as follows: Note that the classical analysis of the RG-flow is determined by the asymptotic behavior of *real* poles in the complex- z plane after a Laplace-transformation from t into z -space. For a quantum walk, these Laplace-poles are *complex* and behave in more subtle ways. Those real poles merely flow radially in the complex- z plane, i.e., simply along the real- z axis, impinging on the complex unit-circle only at $z = 1$, whereby the long-time behavior can be discerned [19]. The corresponding complex poles in a quantum walk flow simultaneously in radial and tangential directions, and impinge on the unit circle in increasingly dense bands. The key observation in this paper is that the corresponding radial flow of poles in the quantum walk, albeit dominant, ultimately *cancels* due to unitarity. As a consequence, the otherwise sub-dominant tangential flow of poles actually controls the walk dynamics. Based on this insight, we are able to derive some – but not all – of the previously obtained results analytically. The remaining obstacles indicate that certain systems possess even more intricate scaling behavior than described here.

In the following, we first highlight in Sec. II the properties of a unitary evolution equation, its solution, and its differences with a random walk equation. In Sec. III, we review the generic RG-evaluation of scaling in classical random walks, followed by the corresponding derivation for quantum walks. In Sec. IIIB, we apply the results of the preceding RG-analysis to the specific cases of the known quantum walks on fractals. We conclude with a discussion of the results in Sec. IV.

II. UNITARY EVOLUTION EQUATIONS

We consider the evolution equation for a classical or quantum walk that is discrete in time and space,

$$\Psi(\vec{x}, t+1) = \sum_{\vec{y}} \mathcal{U}(\vec{x}, \vec{y}) \Psi(\vec{y}, t), \quad (2)$$

where the propagator $\mathcal{U}(\vec{x}, \vec{y})$ is some $M \times M$ matrix with M reflecting a combination of a discrete set of N

lattice sites and possibly a certain number of internal degrees of freedom at each site. Assuming that we possess the eigensolution for the propagator, $\mathcal{U}\phi_j = u_j\phi_j$ with an orthonormal set of eigenvectors $\{\phi_j(\vec{x})\}_{j=1}^M$, then the formal solution of Eq. (2) becomes

$$\Psi(\vec{x}, t) = \sum_{\vec{y}} \mathcal{U}^t(\vec{x}, \vec{y}) \Psi(\vec{y}, 0) = \sum_{j=1}^M a_j u_j^t \phi_j(\vec{x}). \quad (3)$$

For a classical random walk, the site amplitude itself provides the probability density, $\rho(\vec{x}, t) = \Psi(\vec{x}, t)$, while for the quantum walk it is $\rho(\vec{x}, t) = |\Psi(\vec{x}, t)|^2$. To preserve the norm $\sum_{\vec{x}} \rho(\vec{x}, t) \equiv 1$, the propagator \mathcal{U} is stochastic for a random walk, while it must be *unitary* for a quantum walk. For the stochastic operator of a random walk, aside from the unique (+1)-eigenvalue of the stationary state, the remaining eigenvalues have $|u_j| < 1$, thus, according to Eq. (3), the dynamics is determined by $\rho(\vec{x}, t) \sim e^{-\epsilon t}$ for large times t with $\epsilon = -\ln \max\{|u_j| < 1; 1 \leq j \leq M\}$. In turn, for unitary \mathcal{U} all eigenvalues are uni-modular, $|u_j| = 1$, such that $u_j = e^{i\theta_j}$ with real θ_j . Then,

$$\rho(\vec{x}, t) = r(\vec{x}) + \sum_{l < j}^M s_{j,l}(\vec{x}) \cos[(\theta_j - \theta_l)t], \quad (4)$$

where r, s only depend on position and initial conditions. The cut-off relevant for the long-time asymptotic behavior here is provided by $\Delta\theta = \min\{|\theta_j - \theta_l| > 0; 1 \leq j, l \leq M\}$. Furthermore, we note that a discrete Laplace transform (or generating function),

$$\bar{\Psi}(\vec{x}, z) = \sum_{t=0}^{\infty} \Psi(\vec{x}, t) z^t, \quad (5)$$

of Eq. (4) provides

$$\bar{\rho}(\vec{x}, z) = \frac{C(\vec{x})}{\prod_{j,l}^M [1 - z e^{i(\theta_j - \theta_l)}]}, \quad (6)$$

after placing all terms in the transformation of Eq. (4) on their main denominator. Thus, all poles of $\bar{\rho}(\vec{x}, z)$ in Eq. (6), and hence for the site amplitudes $\bar{\Psi}(\vec{x}, z)$, are located right on the unit-circle in the complex- z plane.

III. RENORMALIZATION GROUP FOR WALKS

Instead of providing specific examples of walks on certain networks here, we merely recount the essential details that allow us to efficiently frame the RG analysis, its problem for quantum walks, and how we propose to resolve it. An explicit derivation for the pedagogical case of a walk on a 1d-line, for example, in parallel for the classical and the quantum case, can be found in Ref. [34].

To apply the renormalization group to a walk problem [19], it is convenient to eliminate time t in the evolution equation, Eq. (2), in the site basis via the discrete Laplace transform in Eq. (5). Assuming a walk with an initial condition at $t = 0$ that is localized at the origin, we get

$$\bar{\Psi}(\vec{x}, z) = \sum_{\vec{y}} z \mathcal{U}(\vec{x}, \vec{y}) \bar{\Psi}(\vec{y}, z) + \delta_{\vec{x}, 0} \psi_{IC}. \quad (7)$$

On exactly renormalizable networks, this linear system of equations can now be decimated recursively by algebraically eliminating specific site amplitudes such that the system remains self-similar after each iteration [15, 16]. Typically, this requires the matrix $z\mathcal{U}$ to be sparse and its non-zero coefficients should be re-presentable in terms of just a small set $\vec{a}_0(z) = (a_0, b_0, c_0, \dots)$ of site-independent “hopping parameters” of the unrenormalized state. Each iteration constitutes an RG-step from level k to $k + 1$, starting at the unrenormalized state with $k = 0$. Each RG-step represents a coarse-graining of the system, such that each remaining amplitude at level k represents a spatial domain of length $L = b^k$, and the \vec{a}_k the effective transitions between those, where b is the rescaling of length in each step. (It is $b = 2$ in most cases referred to here.) These “renormalized” \vec{a}_k arise, as the remaining equations attain self-similarity only for an appropriate redefinition of the hopping parameters, leading to the mapping

$$\vec{a}_{k+1}(z) = \mathcal{RG}[\vec{a}_k(z)]. \quad (8)$$

which is called the RG-flow. This set of coupled, rational maps exactly encapsulates the entire walk process.

While the RG-flow in Eq. (8) usually can not be solved in general, the properties of its fixed point(s)

$$\vec{a}_\infty = \mathcal{RG}(\vec{a}_\infty) \quad (9)$$

for $k \rightarrow \infty$ can be explored to reveal the dynamics of the walk asymptotically at large length- and time-scales. Specifically, $k \rightarrow \infty$ corresponds to a diverging system size $N = L^{d_f}$ while $|z| \rightarrow 1$ according to Eq. (5) accesses the large- t limit, as the hopping parameters $\vec{a}_k(z)$ become ever-more complicated rational functions in z under the RG-flow in Eq. (8). We can linearize the RG-flow via the Ansatz

$$\vec{a}_k(z) \sim \vec{a}_\infty + (1 - z)\vec{\alpha}_k, \quad (10)$$

for $z \rightarrow 1$ and $k \rightarrow \infty$, assuming $(1 - z)\vec{\alpha}_k \ll 1$. Then, we get the linear system

$$\vec{\alpha}_{k+1} = \vec{\alpha}_k \circ J, \quad (11)$$

with the Jacobian matrix

$$J = \left(\frac{\partial \mathcal{RG}}{\partial \vec{a}_k} \Big|_{k \rightarrow \infty} \right), \quad (12)$$

such that the solutions of Eq. (11) are linear combinations,

$$\vec{\alpha}_k \sim \lambda_1^k \vec{v}_1 \mathcal{A}_1 + \lambda_2^k \vec{v}_2 \mathcal{A}_2 + \dots, \quad (13)$$

where λ_j are the eigenvalues of J in descending order, and \vec{v}_j the associated eigenvectors. (Since J is not necessarily Hermitian, the eigenvectors are not necessarily orthogonal!)

As Sec. II suggests, especially the Laplace-poles closest to $|z| \rightarrow 1$ assume an important role. Now, the location of the poles in the complex- z plane for any observable, like the PDF $\bar{p}(\vec{x}, z)$, do not necessarily correspond to those of $\vec{a}_k(z)$, although $\bar{p}(\vec{x}, z) = f_{\vec{x}}[\vec{a}_k(z)]$ is a *functional* of the hopping parameters. However, this distinction does not pose a problem for the real poles in the classical walk: either set of poles flows radially along the real- z axis towards $z = 1$, exhibiting the same scaling. In contrast, quantum-walk observables are unitary and therefore have strictly uni-modular poles, such as in Eq. (6), that flow only tangentially on the unit circle in the complex- z plane, while the renormalized hopping parameters $\vec{a}_k(z)$ individually have poles that flow radially *and* tangentially, with no obvious connection a-priori, see Fig. 1. In the following, we explore this distinction.

A. Classical Fixed-Point Analysis

For a classical random walk, almost all poles of $\vec{a}_k(z)$ are on the real- z axis with $z > 1$. Let z_k be the pole that is closest to $z = 1$, to wit,

$$z_k \sim 1 + \epsilon_k, \quad (\epsilon_k \rightarrow 0) \quad (14)$$

with real $\epsilon_k > 0$. Then, the generic form for a simple pole near $z = 1$, with $\vec{a}_k(1) = \vec{a}_\infty$ at the fixed point in Eq. (9), is:

$$\vec{a}_k(z) \sim \frac{1 - z_k}{z - z_k} \vec{a}_\infty \sim \vec{a}_\infty \left[1 - \frac{1}{\epsilon_k} (1 - z) + \dots \right], \quad (15)$$

which is the expected behavior for the hopping parameters that justifies the Ansatz in Eq. (10). Note that $1/\epsilon_k$ is not only the most divergent term of order $1 - z$, it is the only divergence possible. This is reflected in Eq. (13) in the fact that there is only a single divergent eigenvalue, $\lambda_1 > 1$, of the Jacobian in Eq. (12) for a classical walk. The comparison implies

$$\epsilon_k \sim |\vec{\alpha}_k|^{-1} \sim \lambda_1^{-k} \quad (16)$$

at the cross-over $(1 - z)\alpha_k \sim 1$ that determines the cut-off.

With $\bar{p}(\vec{x}, z) = f_{\vec{x}}[\vec{a}_k(z)]$, the classical PDF now attains the form for $z \rightarrow 1$:

$$\bar{p}(\vec{x}, z) \sim \frac{1 - z'_k}{z - z'_k} A, \quad (17)$$

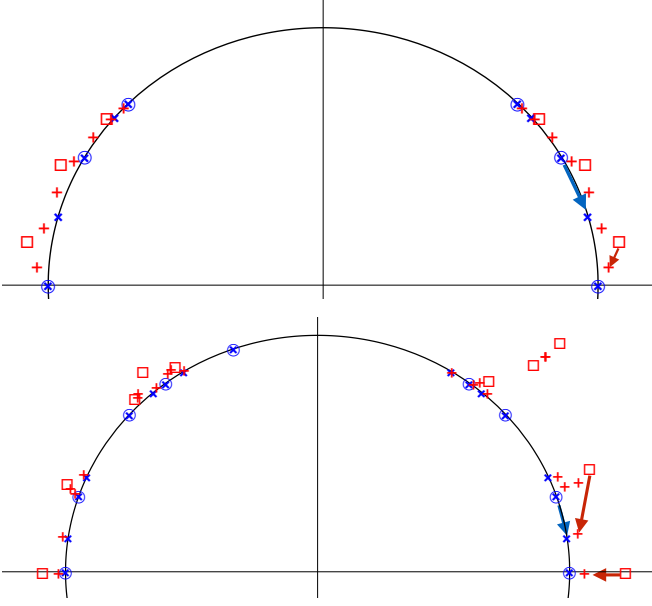


Figure 1. Plot of the poles of the Laplace transforms in the complex- z plane at RG-steps $k = 2$ and $k = 3$ for some site-amplitude $\bar{\psi}_0^{(k)}(z)$ (in blue, with \circ for $k = 2$ and \times for $k = 3$) and for the hopping parameters $\bar{a}_k(z)$ (in red, with \square for $k = 2$ and $+$ for $k = 3$) for quantum walk on the 1d-line (top) and the dual Sierpinski gasket (bottom). (In these walks, poles are certain to occur in complex-conjugate pairs, so only the upper z -plane is shown.) Even at such small orders k , there is a large number of poles, which proliferate exponentially with k . All poles for the site-amplitude are on the unit-circle, while all poles for the hopping parameters are outside. Although the pattern by which poles evolve appears complicated, either type of poles impinge increasingly on the real- z axis. Especially marked is the RG-flow of the poles closest to $z = 1$, both for the site-amplitude (blue arrows) and the hopping parameters (red arrows). While the former only flow tangentially along the circle, the later displace tangentially as well as radially, with one pole potentially flowing just radially inward along the real axis (bottom panel).

where its closest pole $z'_k \sim 1 + C\epsilon_k$ may differ from z_k , but only by a constant C that does not affect the scaling. To see this, we consider the inverse Laplace transform and inserting Eq. (17):

$$\rho(\vec{x}, t) = \oint \frac{dz}{2\pi iz} z^{-t} \bar{\rho}(\vec{x}, z) \sim AC\epsilon_k e^{-C\epsilon_k t}, \quad (18)$$

where ϵ_k provides the cut-off. If we now calculate temporal moments, say, of the first passage time at some site \vec{x} [19], it is

$$\langle t^n \rangle_k = \frac{1}{\mathcal{N}} \int_0^\infty dt t^n \rho(\vec{x}, t) \sim \epsilon_k^{-n}, \quad (19)$$

where the norm \mathcal{N} absorbs any factor so that $\langle t^0 \rangle_k \equiv 1$. Then, Eq. (16) implies for the scaling of the characteristic time-scale T of the dynamics associated with system size

N that

$$T = [\langle t^n \rangle_k]_n^{\frac{1}{n}} \sim \epsilon_k^{-1} \sim \lambda_1^k \sim (2^k)^{\log_2 \lambda_1} \sim L^{d_w} \sim N^{\frac{d_w}{d_f}}, \quad (20)$$

such that the classical walk dimension becomes

$$d_w^{RW} = \log_2 \lambda_1. \quad (21)$$

B. Fixed-Point Analysis of the Quantum Walk

For the quantum walk, Fig. 1 suggests that the poles of the hopping parameters reside in certain bands near but not on the unit circle of the complex- z plane. (All poles come in complex-conjugate pairs for a unitary quantum walk with a purely real coin, such as the Grover coin [35].) As for the classical walk, we shall assume that poles closest to $z = \pm 1$, i.e., those on or near the real- z axis, are again the most relevant. This assumption will prove appropriate but more difficult to justify than in the classical case, as we will discuss below. The key observation now is that the flow of these poles in radial and tangential directions can be parametrized as

$$z_k^{(\pm)} \sim (1 + \epsilon_k) e^{\pm i\theta_k} \sim 1 \pm i\theta_k + \epsilon_k, \quad (1 \gg \theta_k \gg \epsilon_k \gg \theta_k^2) \quad (22)$$

for large order k in the RG-flow, Eq. (8), while there also might be a real pole, $z_k^{(0)} \sim 1 + \epsilon_k$. Previous discussions [15, 16] suggest that radial flow is faster than tangential flow ($\theta_k \gg \epsilon_k$) for these poles. This follows from the scaling collapse found in Refs. [15, 16] that lines up diverging features (i.e., poles close to the unit circle) in the tangential (θ_k) direction, while their width (corresponding to the radial proximity to the circle, measured by ϵ_k) declines more rapidly.

Then, like in Eq. (15) for the classical case, the most generic expression for any hopping parameter is:

$$\bar{a}_k(z) \sim \bar{a}_\infty \left[\frac{pe^{i\phi}}{2\cos\phi} \frac{1 - z_k^{(+)}}{z - z_k^{(+)}} + \frac{pe^{-i\phi}}{2\cos\phi} \frac{1 - z_k^{(-)}}{z - z_k^{(-)}} + (1-p) \frac{1 - z_k^{(0)}}{z - z_k^{(0)}} \right] \quad (23)$$

with possibly ($p < 1$) a real pole at $z_k^{(0)}$ and complex conjugate poles at $z_k^{(\pm)} = [z_k^{(\mp)}]^*$. Note that again $\bar{a}_k(1) = \bar{a}_\infty$ at the fixed point, but that we also assume $\bar{a}_k(z^*) = [\bar{a}_k(z)]^*$. Here, p determines the balance in weight between real and complex roots, while $\phi \neq 0$ allows for a complex residue at the pole. Expanding similar to Eq. (15) for the classical case, we find

$$\bar{a}_k(z) \sim \bar{a}_\infty \left(1 - \left[\frac{r}{\epsilon_k} + s \begin{cases} \frac{\epsilon_k}{\theta_k^2}, & \phi = 0, \\ \frac{1}{\theta_k}, & \phi \neq 0 \end{cases} (1 - z) + \dots \right] \right), \quad (24)$$

with some constants r, s . Thus, allowing for the tangential flow in Eq. (22) produces a second independent divergence at order $1 - z$ in Eq. (24). Hence, we expect both, leading and sub-leading eigenvalues $\lambda_{1,2} > 1$ in Eq. (13) for the respective expansion near the fixed point, to match up with Eq. (24). As in the classical case, Eq. (16), it is typically $\epsilon_k \sim \lambda_1^{-k}$ as the most-divergent contribution in Eq. (24), although interchanging the roles of $\lambda_{1,2}$ does not affect the following outcome: Comparing Eq. (24) with Eq. (13) assuming real residues ($\phi = 0$), it is $\epsilon_k/\theta_k^2 \sim \lambda_2^k$, i.e.,

$$\theta_k \sim \left(\sqrt{\lambda_1 \lambda_2} \right)^{-k}. \quad (25)$$

IV. DISCUSSION

While it would seem futile to consider a subdominant contribution to scaling, we have shown that, due to unitarity, it actually becomes the key to understand the long-range dynamics of a quantum walk. We know that there is a functional relation between the hopping parameters and the PDF, $\bar{p}(\vec{x}, z) = f_{\vec{x}}[\vec{a}_k(z)]$, and we are *assured* by Eq. (6) that all the poles of the PDF are (products of) uni-modular modes. Therefore, the functional must be such that the leading scaling resulting from the radial flow of poles in $\vec{a}_k(z)$ will cancel in the PDF. This fact, as exhibited in Fig. 1, we show explicitly for the case of the quantum walk on a line in the Appendix below. Again, it is guaranteed to occur due to Eq. (6) but a general proof would be useful.

As Eq. (6) further suggests, however, it would appear that it is not sufficient to merely focus on those poles closest to the real- z axis with the smallest θ_k . After all, it is the smallest *difference* $\Delta\theta$ in the arg of two poles that sets the cut-off. But we will now argue that there should be only *one* scale, θ_k as in Eq. (25), for the tangential flow of poles: Poles anywhere along the unit circle either (1) scale with θ_k , like those closest to the real axis, or (2) may converge to some complex constant, in which case their correction scales like θ_k . Under that assumption, $\Delta\theta$ is either the difference of two type-(1) poles, two type-(2) poles, or a type-(1) and a type-(2) pole. The first case again leads to θ_k itself again, the second case either leads to another constant or, if the two leading constants of the type-(2) poles cancel, it leads back to the first case, and the third case merely converges to the constant part of the type-(2) pole. Consequently, we find a minimal $\Delta\theta \sim \theta_k$, even if the poles that contribute to the smallest difference are not those closest to the real- z axis and the fixed point there. Yet, observing these poles *does* provide the relevant scaling, θ_k in Eq. (25).

To justify these conclusions, we can re-assess some of the previous results and the conjecture of $d_w^{QW} = \frac{1}{2} d_w^{RW}$ [15, 16]. The easiest case of quantum walk on a 1d-

line, in which all hopping parameters and any observable can be calculated not only asymptotically but also in closed form, unfortunately does not provide much insight here: The RG analysis [34] yields degenerate Jacobian eigenvalues, $\lambda_1 = \lambda_2 = 2$, such that there is no distinction, i.e., $\lambda_1 \equiv \sqrt{\lambda_1 \lambda_2}$, and one would be lead to the false conclusion that a naive classical analysis as in Sec. III A would suffice. In this case, we can merely ascertain (in the Appendix) that the tangential flow of poles in the hopping parameters translates exactly into that of the poles belonging to observable while the radial flow cancels. Although this can not be shown generally but only for small system sizes in the non-trivial fractal networks, these in turn allow to validate Eq. (25): The RG for quantum walk on the dual Sierpinski gasket (DSG) [15] yields $\lambda_1 = 3$, $\lambda_2 = \frac{5}{3}$, and $\lambda_3 = 1$, such that $\sqrt{\lambda_1 \lambda_2} = \sqrt{5}$ provides the numerically determined scaling, $d_w^{QW} = \log_2 \sqrt{5}$, and $\lambda_3 \neq 1$ remains irrelevant. Since classically $\lambda_1^{RW} = 5$, it verifies the conjecture of $d_w^{QW} = \frac{1}{2} d_w^{RW}$. The same pattern holds for the two Migdal-Kadanoff networks analyzed in Ref. [16]: For the 3-regular network called MK3, the Jacobian eigenvalues are $\lambda_1 = 7$ and $\lambda_2 = 3$ such that $\lambda_1 \lambda_2 = \lambda_1^{RW} = 21$, and for the 4-regular network called MK4 they are $\lambda_1 = 13$ and $\lambda_2 = \frac{19}{7}$, such that $\lambda_1 \lambda_2 = \lambda_1^{RW} = \frac{247}{7}$. It is surprising, then, that for the 3-regular Hanoi network called HN3 [36], Ref. [16] found $\lambda_1 = 2$ and $\lambda_2 = (1 + \sqrt{17})/4$, so that $\lambda_1 \lambda_2 \neq \lambda_1^{RW} = 2(\sqrt{5} - 1)$ is unrelated to the classical eigenvalue, yet, numerically the conjecture still appears to hold. This suggests that the relation in Eq. (25) is not quite so fundamental, i.e., some of the assumptions leading to it are violated by HN3. Not even the simple alternative of complex residues at the poles, $\phi \neq 0$ in Eq. (24), implying $\theta_k \sim \lambda_2^{-k}$, can explain the discrepancy. Furthermore, it appears that a more general argument than Eq. (25) must exist to justify the conjecture $d_w^{QW} = \frac{1}{2} d_w^{RW}$. Finally, we note in passing that in all cases of quantum walks, the dominant Jacobian eigenvalue happens to provide the fractal exponent of the network itself, $\log_2 \lambda_1 = d_f$.

Acknowledgements: SB and SL acknowledge financial support from the U. S. National Science Foundation through grant DMR-1207431. SB acknowledges financial support from CNPq through the “Ciência sem Fronteiras” program. SL acknowledges financial support from the American Physical Society through the Brazil-U.S. Exchange Program. Both, SB and SL thank LNCC for its hospitality. RP acknowledges financial support from Faperj and CNPq.

-
- [1] L. K. Grover, Phys. Rev. Lett. **79**, 325 (1997).
 - [2] A. M. Childs and J. Goldstone, Phys. Rev. A **70**, 022314 (2004).

- [3] A. Ambainis, J. Kempe, and A. Rivosh, in *Proceedings of the sixteenth annual ACM-SIAM symposium on Discrete algorithms*, SODA '05 (Society for Industrial and Applied Mathematics, Philadelphia, PA, USA, 2005) pp. 1099–1108.
- [4] A. Ambainis, R. Portugal, and N. Nahimov, *Quantum Information & Computation* **15**, 1233 (2015).
- [5] S. Li and S. Boettcher, *Phys. Rev. A* (to appear, arXiv:1607.05317).
- [6] P. W. Shor, *Proc. 35th Annual Symposium on Foundations of Computer Science* (1994).
- [7] C. Moore and S. Mertens, *The Nature of Computation* (Oxford University Press, Oxford, 2011).
- [8] G. D. Paparo, M. Müller, F. Comellas, and M. A. Martin-Delgado, *Sci. Rep.* **3**, 2773 (2013).
- [9] S. Chakraborty, L. Novo, A. Ambainis, and Y. Omar, *Phys. Rev. Lett.* **116**, 100501 (2016).
- [10] R. Motwani and P. Raghavan, *Randomized Algorithms* (Cambridge University Press, 1995).
- [11] A. M. Childs, *Phys. Rev. Lett.* **102**, 180501 (2009).
- [12] A. M. Childs, D. Gosset, and Z. Webb, *Science* **339**, 791 (2013).
- [13] N. Inui, N. Konno, and E. Segawa, *Phys. Rev. E* **72**, 056112 (2005).
- [14] S. Falkner and S. Boettcher, *Phys. Rev. A* **90**, 012307 (2014).
- [15] S. Boettcher, S. Falkner, and R. Portugal, *Phys. Rev. A* **90**, 032324 (2014).
- [16] S. Boettcher, S. Falkner, and R. Portugal, *Phys. Rev. A* **91**, 052330 (2015).
- [17] Y. Ide, N. Konno, E. Segawa, and X.-P. Xu, *Entropy* **16**, 1501 (2014).
- [18] G. H. Weiss, *Aspects and Applications of the Random Walk* (North-Holland, Amsterdam, 1994).
- [19] S. Redner, *A Guide to First-Passage Processes* (Cambridge University Press, Cambridge, 2001).
- [20] H. B. Perets, Y. Lahini, F. Pozzi, M. Sorel, R. Morandotti, and Y. Silberberg, *Phys. Rev. Lett.* **100**, 170506 (2008).
- [21] L. Martin, G. D. Giuseppe, A. Perez-Leija, R. Keil, F. Dreisow, M. Heinrich, S. Nolte, A. Szameit, A. F. Abouraddy, D. N. Christodoulides, and B. E. A. Saleh, *Opt. Express* **19**, 13636 (2011).
- [22] L. Sansoni, F. Sciarrino, G. Vallone, P. Mataloni, A. Crespi, R. Ramponi, and R. Osellame, *Phys. Rev. Lett.* **108**, 010502 (2012).
- [23] A. Crespi, R. Osellame, R. Ramponi, V. Giovannetti, R. Fazio, L. Sansoni, F. D. Nicola, F. Sciarrino, and P. Mataloni, *Nature Photonics* **7**, 322 (2013).
- [24] C. Weitenberg, M. Endres, J. F. Sherson, M. Cheneau, P. Schauss, T. Fukuhara, I. Bloch, and S. Kuhr, *Nature* **471**, 319 (2011).
- [25] S. Havlin and D. Ben-Avraham, *Adv. Phys.* **36**, 695 (1987).
- [26] J.-P. Bouchaud and A. Georges, *Phys. Rep.* **195**, 127 (1990).
- [27] B. D. Hughes, *Random Walks and Random Environments* (Oxford University Press, Oxford, 1996).
- [28] S. Condamin, O. Benichou, V. Tejedor, R. Voituriez, and J. Klafter, *Nature* **450**, 77 (2007).
- [29] S. Boettcher and B. Gonçalves, *Europhysics Letters* **84**, 30002 (2008).
- [30] N. Konno, *Quantum Information Processing* **1**, 345 (2002).
- [31] G. Grimmett, S. Janson, and P. F. Scudo, *Physical Review E* **69**, 026119+ (2004).
- [32] K. G. Wilson, *Phys. Rev. B* **4**, 3174 (1971).
- [33] R. K. Pathria, *Statistical Mechanics*, 2nd Ed. (Butterworth-Heinemann, Boston, 1996).
- [34] S. Boettcher, S. Falkner, and R. Portugal, *Journal of Physics: Conference Series* **473**, 012018 (2013).
- [35] R. Portugal, *Quantum Walks and Search Algorithms* (Springer, Berlin, 2013).
- [36] S. Boettcher, B. Gonçalves, and H. Guclu, *J. Phys. A: Math. Theor.* **41**, 252001 (2008).

APPENDIX

Poles of Hopping Parameters and Observables

Here we show that poles in Laplace-space for the hopping parameters can not be on the unit circle of the complex- z plane, while in turn the poles of the site-amplitudes are *only* on that circle, as shown in Fig. 1. While this holds for any system due to Eq. (6), we demonstrate this here by example of a quantum walk on a 1d-line with periodic boundary conditions.

The propagator \mathcal{U} on the 1d-line is given by

$$\mathcal{U} = \sum_n \{A \delta_{n,n+1} + B \delta_{n,n-1} + M \delta_{n,n}\}, \quad (26)$$

where the general form of the hopping operators A , B , and M is only constrained by the requirement of unitarity:

$$\begin{aligned} \mathcal{I} &= \mathcal{U}^\dagger \mathcal{U}, \\ &= \sum_n \sum_m \{A^\dagger \delta_{n,n+1} + B^\dagger \delta_{n,n-1} + M^\dagger \delta_{n,n}\} \\ &\quad \{A \delta_{m,m+1} + B \delta_{m,m-1} + M \delta_{m,m}\}, \\ &= \sum_n \{ (A^\dagger A + B^\dagger B + M^\dagger M) \delta_{n,n} + (A^\dagger M + M^\dagger B) \delta_{n,n+1} \\ &\quad + (B^\dagger M + M^\dagger A) \delta_{n,n-1} + A^\dagger B \delta_{n,n+2} + B^\dagger A \delta_{n,n-2} \}, \end{aligned} \quad (27)$$

which is satisfied by the hopping matrices:

$$\begin{aligned} \mathcal{I} &= A^\dagger A + B^\dagger B + M^\dagger M, \\ 0 &= A^\dagger M + M^\dagger B = (B^\dagger M + M^\dagger A)^\dagger, \\ 0 &= A^\dagger B = (B^\dagger A)^\dagger. \end{aligned} \quad (28)$$

Adding these relations implies that the sum $A + B + M$ itself is unitary. Due to the self-similarity of any renormalized structure, this property will remain true after each RG-step k . For example, from Eq. (7) applied to Eq. (26), we learn that in Laplace-space the hopping parameters at the initial ($k = 0$) RG-step have the form $A_0 = zA$, $B_0 = zB$, and $M_0 = zM$ and subsequently become complicated algebraic expressions of z via the RG-flow in Eq. (8). Then, while on the unit circle in the

complex- z plane, we have at any k that

$$\det[A_k(z) + B_k(z) + M_k(z)] = e^{i\xi_k(z)} \quad (|z| = 1) \quad (29)$$

with some real phase $\xi_k(z)$.

Poles of the renormalized hopping parameters

While the conditions in Eq. (28) are more generally valid for any r -dimensional matrices with $r \geq 2$, we restrict ourselves to the simplest case $r = 2$. The renormalization group treatment of the quantum walk on the $1d$ -line [34] entails a decomposition of the hopping matrices into the unitary 2×2 coin matrix \mathcal{C} and k -th renormalized shift matrices

$$P_k = \begin{pmatrix} a_k & 0 \\ 0 & 0 \end{pmatrix}, \quad Q_k = \begin{pmatrix} 0 & 0 \\ 0 & -a_k \end{pmatrix}, \quad R_k = \begin{pmatrix} 0 & b_k \\ b_k & 0 \end{pmatrix}, \quad (30)$$

such that $A_k = P_k \mathcal{C}$, $B_k = Q_k \mathcal{C}$, and $M_k = R_k \mathcal{C}$. Here, $a_k(z)$ and $b_k(z)$ are the scalar renormalized hopping parameters that obey an RG-flow as described in Eq. (8). (For the explicit form, of these recursions, see Ref. [34].) Since the coin \mathcal{C} is unitary, the shift matrices then must satisfy the same conditions in Eq. (28). While the last two relations are satisfied automatically for matrices in the form of Eq. (30), the first relation implies that

$$|a_k(z)|^2 + |b_k(z)|^2 = 1 \quad (|z| = 1). \quad (31)$$

This proves that neither a_k nor b_k can have any singularities on the unit circle $|z| = 1$.

We finally remark that Eq. (31) in itself does not imply that there is a constraint between a_k and b_k that could make one of these redundant. Eq. (31) fixes their relation only up to a phase that could itself depend on k and z .

For example, the alternative unitarity condition derived from Eq. (29) would say:

$$a_k^2(z) + b_k^2(z) = e^{i\xi_k(z)}. \quad (32)$$

Poles of the site amplitudes

Although we have already shown in Eq. (6) on very general grounds that the poles of the site-amplitudes are all located on the unit-circle in the complex- z plane, it is quite instructive to see how this fact emerges in each particular case, especially in relation with the hopping parameters. In our example of the $1d$ -line of $N = 2^k$ sites with periodic boundary conditions, the loop merely consists of four remaining sites after $k-2$ RG-steps, with

$$\begin{aligned} \bar{\psi}_0 &= A_{k-2} \bar{\psi}_{\frac{N}{4}} + B_{k-2} \bar{\psi}_{\frac{3N}{4}} + M_{k-2} \bar{\psi}_0 + \psi_{IC}, \\ \bar{\psi}_{\frac{N}{4}} &= A_{k-2} \bar{\psi}_{\frac{N}{2}} + B_{k-2} \bar{\psi}_0 + M_{k-2} \bar{\psi}_{\frac{N}{4}}, \\ \bar{\psi}_{\frac{N}{2}} &= A_{k-2} \bar{\psi}_{\frac{3N}{4}} + B_{k-2} \bar{\psi}_{\frac{N}{4}} + M_{k-2} \bar{\psi}_{\frac{N}{2}}, \\ \bar{\psi}_{\frac{3N}{4}} &= A_{k-2} \bar{\psi}_0 + B_{k-2} \bar{\psi}_{\frac{N}{2}} + M_{k-2} \bar{\psi}_{\frac{3N}{4}}. \end{aligned} \quad (33)$$

Then, focusing on the amplitude for the site where the quantum walk initiated, we obtain after some algebra,

$$\bar{\psi}_0 = [\mathbb{I} - (A_k + B_k + M_k)]^{-1} \psi_{IC}. \quad (34)$$

Since $A_k + B_k + M_k$ is a unitary matrix for $|z| = 1$, with an orthonormal set of eigenfunctions and eigenvalues as a function of z , we can expand the matrix on the right-hand side of Eq. (34) in those eigenfunctions and obtain the poles of $\bar{\psi}_0$ whenever one (or more) of its eigenvalues become $= 1$ for some value of z . We have obtained expressions equivalent to Eq. (34) for other fractal networks, however, these are lengthy and it is cumbersome to establish the uni-modularity of their poles case-by-case, although it is always ensured by Eq. (6).